



# Study on the difference between in-situ and ex-situ catalytic pyrolysis of oily sludge

Qian He<sup>1,2</sup> · Shengxiong Huang<sup>1,2</sup> · Wei Luo<sup>1,2,3</sup> · Yifeng Su<sup>2,4</sup> · Mao Xia<sup>1,2</sup> · Nan Zhou<sup>1,2</sup> · Zhi Zhou<sup>1,2</sup> 

Received: 25 January 2021 / Accepted: 28 April 2021 / Published online: 7 May 2021

© The Author(s), under exclusive licence to Springer-Verlag GmbH Germany, part of Springer Nature 2021

## Abstract

In-situ catalytic pyrolysis has simple process configuration and low cost. Ex-situ catalytic pyrolysis can optimize the pyrolysis capacity and upgrade catalysis, and the catalytic can be reused. But there have been few studies researched on compare in-situ and ex-situ catalytic pyrolysis of the OS performed in similar reactor with two kinds of catalytic. This paper study the pyrolysis of oily sludge (OS) uses CaO and oily pyrolysis char as catalytic at 700 °C. Through analysis the pyrolysis oil (PO), pyrolysis solid (PS) and pyrolysis gas (PG) during pyrolysis procedure to research the difference between in-situ and ex-situ catalytic pyrolysis. The gas chromatography-mass spectrometry (GC-MS) results show that CaO was conducive to the synthesis of aromatics, which content more than aliphatics and heterocyclics in CaO-i (i: in-situ) and CaO-e (e: ex-situ) groups. However, char greatly inhibits the production of aromatic compounds and promotes the production of aliphatic compounds. Gas chromatography (GC) results present that the char and CaO can greatly increase the content of combustible gas and the content reach to 85.85%, the pyrolysis gas (PG) keep at the highest combustion performance in char-CaO-i group. Meanwhile, compared with uncatalyzed groups, the content of CH<sub>4</sub> and CO increased about 2.05% and 3.93%, respectively. Fourier transform infrared spectroscopy (FT-IR) show that char and CaO reduce the function groups number of pyrolysis solid (PS), and it shows that the pyrolysis reaction is more complete. This research is expecting to provide theory support for catalytic pyrolysis of OS.

**Keywords** Oily sludge · Catalytic pyrolysis · In-situ · Ex-situ

## Introduction

The rapid development of economy and industry are inseparable from the consumption of fossil energy such as oil and gas. During the explored process of fossil energy, large number of Oily sludge (OS) will be produced. OS is a complex mixture which generally consisting of 30–50 wt.% water, 30–80 wt.% oil, and 10–20 wt.% solids

(Abdel Azim, et al. 2011; Huang, et al. 2014). The OS contains a variety of teratogenic and carcinogenic toxic substances, such as heavy metals, benzene, phenols, anthracene, pyrene, and so on (Liu, et al. 2009). Improper disposal of OS is detrimental to human beings and the environment (Cheng, et al. 2017). Due to the complex characteristics of OS, scholars raise various treatment methods including solidification (Karamalidis and Voudrias 2007; Leonard and Stegemann 2010), ultrasonic (Al-Zahrani and Putra 2013; Check and Mowla 2013; Jin, et al. 2012), solvent extraction (Al-Zahrani and Putra 2013; Zubaidy and Abouelnasr 2010), bioremediation (Cameotra and Singh 2008; Mrayyan and Battikhi 2005), landfill, incineration (Hou, et al. 2014; Liu, et al. 2009; Zhou, et al. 2009), and pyrolysis (Shie, et al. 2003; Wang, et al. 2007). Generally speaking, landfill will cause secondary pollution of soil and water, solvent extraction usually consumes a large amount of organic solvents and pollution of the environment, and incineration will consume a large amount of electricity and with high cos (Elektorowicz and Habibi 2005; Hu, et al. 2013; Shie et al., 2004a, b).

Responsible Editor: Santiago V. Luis

✉ Zhi Zhou  
zhouzhi@hunau.edu.cn

<sup>1</sup> School of chemistry and materials science, Hunan Agricultural University, Changsha 410128, China

<sup>2</sup> Hunan Engineering Research Center for Biochar, Hunan Agricultural University, Changsha 410128, China

<sup>3</sup> Powder Metallurgy Research Institute, Central South University, Changsha 410083, China

<sup>4</sup> College of resources and environment, Hunan Agricultural University, Changsha 410128, China

Up to now, pyrolysis is a promising method to recycle resources from OS (Egazar'yants, et al. 2015). Pyrolysis of OS at temperatures is ranging usually from 100 to 800 °C in an inert atmosphere (e.g., CO<sub>2</sub> and N<sub>2</sub>). It is easily to obtain of pyrolysis solid (PS), pyrolysis oil (PO), and pyrolysis gas (PG) products and emits fewer air pollutants (e.g., NO<sub>x</sub> and SO<sub>2</sub>) compared to combustion. Moreover, after pyrolysis, the heavy metals can be retained in PS, and the PO and PG products can be reprocessed into fuels and chemicals (Song, et al. 2018; Wu et al., 2019a, b). So, the application of OS pyrolysis is identified as an efficient way to promote economic sustainable development and waste value-added utilization (Salman, et al. 2017; Wu et al., 2019a, b). However, it has been reported that the oil sludge is a kind of fuel with high volatile content and low heat value. Its main heat release is caused by the uniform combustion of volatiles matter. The pyrolysis will lead to unstable combustion without catalytic during the process. Lu et al. (2015) investigated that with the increase of pyrolysis temperature, the heavy metal content in biochar would increase significantly due to enrichment at non-catalytic condition. Jin et al. (2016) found that most of the heavy metals exist in the oxidizable and residual forms after pyrolysis, especially at 600 °C. This would result in a significant decline in bioavailability and leading to a very low ecological risk of biochar exposed to the environment.

In addition, it is found that catalytic affect the pyrolysis process of OS, such as the production yield of different phase. In recent years, as a kind of carbon-based catalysts, char has been widely used in the pyrolysis reforming of organic compounds. The researchers believe that metal-containing char is more active than metal-none char in terms of catalytic activity of gasification; it can promote PO cracking and volatile reforming (Fuentes-Cano, et al. 2013; Min, et al. 2011; Wang, et al. 2011). Some researchers studied the influence mechanism of char on PO and found that the presence of alkali and alkaline earth metals (AAEMs) could promote the secondary cracking of heavy PO and improve the quality of PO (Wang et al., 2017a, b; Zhao, et al. 2019; Zhao, et al. 2018). However, purchase char which containing precious metals is expensive, difficult and hard to treat the residue. In addition, catalytic reforming processes are carried out at higher temperatures helpful to ensure adequate levels of PO cracking, which may result in the evaporation of some AAEMs to the gaseous state (Gilbert, et al. 2009; Shen, et al. 2015; Zhang, et al. 2013). So, researchers are more and more interested in using cheap AAEMs as catalyst, such as calcium-based catalyst (Iliopoulou, et al. 2012; Yang, et al. 2019). Shie et al. (2003); 2004a, b) researched the effect of calcium-based catalyst on oil products from catalytic pyrolysis of sludge, and the results showed that Ca species improved the quality of PO. Chen et al. (2017) studied the influence of CaO on PO composition of different pyrolysis objects, the results showed that CaO could reduce the yield of PO, and the concentration of

organic acids in PO would decrease with the increase of CaO content. The presence of Ca has a significant influence on the distribution of pyrolysis products, but its activity is greatly affected by pyrolysis temperature.

However, there have been few studies researched on compare in-situ and ex-situ catalytic pyrolysis of the OS performed in similar reactors with two kinds of catalytic. In this study, the formation mechanism of three phase products (PO, PS, and PG) in in-situ and ex-situ catalytic pyrolysis of sludge was investigated, and the characteristics of the two catalytic methods were compared.

## Material and methods

### Materials

The raw OS sample used in the pyrolysis experiments was taken from Tuha oilfield (Turpan, Xinjiang Uygur Autonomous Region, China), and the moisture content of raw OS was about 26.55 wt.%. Before the experiments, the OS was dried (105 °C for 24 h) and then ground it into a 100 mesh to obtain dry basis OS sample. The proximate and ultimate analysis of dry basis OS are shown in Table 1. The oily pyrolysis char was prepared by pyrolysis of dry basis OS sample at 700 °C without catalyst, and it was also ground into 100 mesh.

### Experimental equipment and conditions

The catalytic pyrolysis experiments were carried out in a horizontal quartz tube fixed-bed reactor system which has two heating stages as shown in Fig. 1. The length of the fixed-bed reactor is 610 mm and the inner diameter is 40 mm, and a perforated plate in the middle of the quartz tube divides it into two zones. In temperature gradient experiments (non-catalyst), 100 g OS was put into the reactor, and 300 mL/min of nitrogen was pumped for 20 min to drain the air out of the reactor before the experiments. Subsequently, the pyrolysis process at a heating rate of 10 °C/min from the room temperature to 600, 650, 700, 750 and 800 °C and maintained for 1 h. Then the flow rate of nitrogen was adjusted to 100 ml/min when the experiments started. In catalytic pyrolysis

**Table 1** The proximate and ultimate analysis of dry basis OS

| Proximate analysis (wt.%) |          |               | Ultimate analysis (wt.%) |      |       |      |      |
|---------------------------|----------|---------------|--------------------------|------|-------|------|------|
| Ash                       | Volatile | Fixed carbon* | C                        | H    | O*    | N    | S    |
| 75.47                     | 17.39    | 7.14          | 63.38                    | 7.25 | 26.71 | 0.32 | 2.34 |

\*By difference

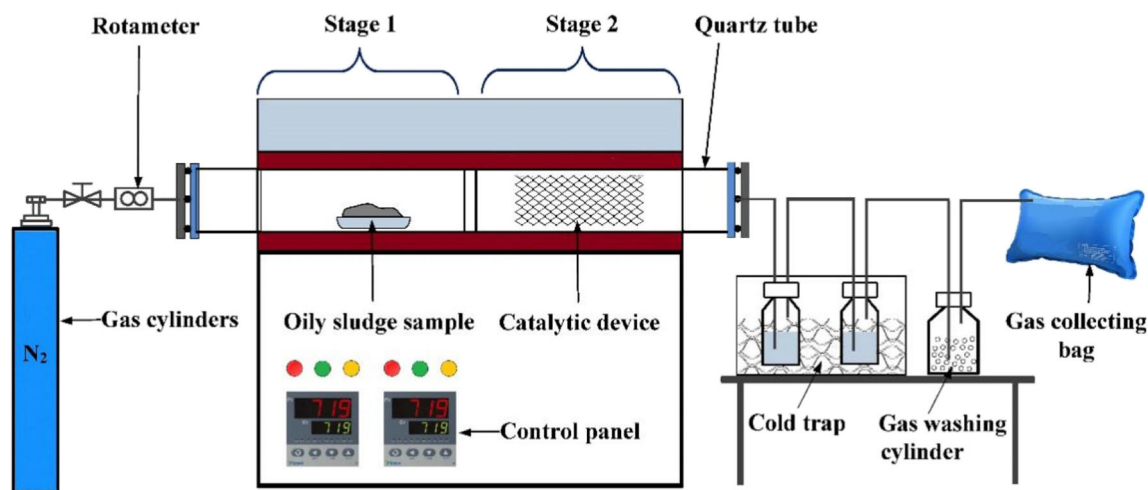


Fig. 1 Horizontal quartz tube fixed-bed reactor system

experiments, 110 g feedstock of OS and catalysts (char or CaO) at a ratio of 10:1 was put into the reactor. As shown in Fig. 1, the OS was placed in the stage 1, the catalyst was dispersed in the porous catalytic device, then the catalytic device was placed in the stage 2, and the pyrolysis temperature of stage 1 and 2 were both kept at 700 °C. The heating rate and nitrogen flow rate of the catalytic pyrolysis experiments were consistent with the temperature gradient experiments. Mixed gas passed through a cold trap and condensable gas was collected in condensate bottles. The non-condensable gas (PG) discharged into the gas collecting bag through gas washing cylinder. After the tube furnace temperature dropped to ambient temperature, the PO from the condensate bottles and the PS from the quartz tank were taken out and weighed by respectively. In the in-situ catalytic pyrolysis experiments, the amount of catalyst was subtracted from the total weight of solid to calculate the amount of PS products. Correspondingly, the gas yield was determined by mass balance. The yield of three phase products from the pyrolysis was calculated as follows.

$$\text{PS yield (wt.\%)} = \frac{\text{mass of solid}}{\text{mass of OS}} \times 100\% \quad (1)$$

$$\text{PO yield (wt.\%)} = \frac{\text{mass of oil}}{\text{mass of OS}} \times 100\% \quad (2)$$

$$\text{PG yield (wt.\%)} = 100\% - \text{PS yield (wt.\%)} - \text{PO yield (wt.\%)} \quad (3)$$

## Analytical methods

The relative content of C, H, O, N, and S in PO were measured by an elemental analyzer (Vario EL cube, Elementar Analysensysteme GmbH, Germany). The components of PO were analyzed by a 6890N- 5975B type GC-MS (Agilent, Agilent Technologies Inc., USA), equipped with a capillary

column (30 m × 0.25 mm inner diameter, with 0.25 μm film thickness, Restek). The GC injector port temperature was 250 °C. The column oven temperature was 80 °C. The ion temperature was 200 °C with a flow split ratio of 30:1. The column oven temperature was increased from 80 to 250 °C at a heating rate of 5 °C/min. The scan mode was scan, the scanned area from m/z 50 to 500, and the solvent interval was 3 min.

The PG was analyzed by GC-5890N gas chromatograph (Nanjing Kejie Analysis Instrument Co. Ltd., China), equipped with a thermal conductivity detector. The pressure of the partial pressure gauge was maintained at 0.3 ~ 0.4 MPa (hold 10 min) and then turn on the instrument the set the oven temperature at 60 °C and the injector temperature maintained at 150 °C and the detector temperature maintained at 100 °C and held for 20 min. Data were acquired and analyzed by N2000 chromatography workstation software.

The PS was detected by Fourier transform infrared spectra analysis (ALPHA, Bruker Corporation, Germany). Take 0.2 g of KBr (Aladdin Chemical Reagent Co., Ltd, Shanghai, China) powder and 1 mg of OS sample and thoroughly grind it in an agate mortar, and the test conditions were as follows: test resolution is 4 cm<sup>-1</sup>, the number of scans was 15 times and the test range were 400–4000 cm<sup>-1</sup>. Data were acquired and analyzed by OPUS software.

## Results and discussion

### Pyrolysis products distribution

PO, PS, and PG were the primary products during OS pyrolysis experiments. The three-phase products distribution in temperature gradient pyrolysis experiments (non-catalyst) was shown in Fig. 2. At 600 °C, the reaction was incomplete, and some volatile components have not been emitted.

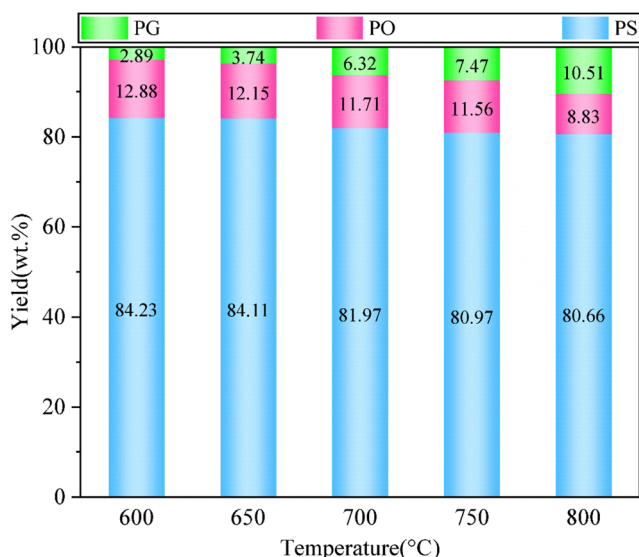


**Fig. 2** The three-phase products distribution in temperature gradient pyrolysis experiments

Therefore, PO and PS had the highest yield, which was 12.88 % and 84.23 %, respectively, while PG had the lowest yield, which was 2.89 %. It is due to that temperature below at 600 °C pyrolysis reaction kept at a lower cracking of heavy hydrocarbon components (C6-C20) (Huang, et al. 2015). With the temperature increased from 600 to 800 °C, the yield of PG was gradually increased, and it reached a maximum (10.50 %), and a decrease in the PO yield was observed. The variation of PS yield was not noticeable, and the result indicated that the PG was mainly attributed to the cracking of the PO (Lin, et al. 2019).

### Pyrolysis oil (PO) characteristics

The components of PO from OS were complex, which were determined by the GC-MS. The PO yields from the uncatalyzed pyrolysis of OS under different temperatures are showed in Fig. 3. To further analyze the components of the pyrolysis oil product, the components of the PO were separated into three fractions (heterocyclics, aliphatics, and aromatics) as shown in Fig. 3a. It shows that the major components of the PO were aromatics; however the content of heterocyclics was low, and the phenomenon was consistent with the other authors (Rodriguez, et al. 2001). This was due to the content of olefins in the OS was mainly, while its oxygen content is relatively low. Furthermore, nitrogen is almost zero, it shown in Fig. 3 b and c shows the influence of temperature on the main 10 principal compounds production during the non-catalytic pyrolysis. As can be seen, the PO were mainly composed of phenol, ketone, monocyclic aromatic hydrocarbons (MAHs), and furan; meanwhile, the total content reached from 80.85% (700 °C) to 89.18% (750 °C). It can be seen from Fig. 3d that the C6-C11 reached a minimum (79.44 %)

at 600 °C and the maximum (85.92%) at 700 °C. As temperature continues to increase from 700 to 800 °C, a little decrease in the C6-C11 was observed.

The molar ratio of H/C reached a maximum (1.32) and the O/C reached a minimum (0.20). Meanwhile, the C6-C11 reached a maximum (85.92%) at 700 °C. Therefore, we continue to choose 700 °C as different pyrolysis conditions to explore the characters of in-situ and ex-situ catalytic pyrolysis.

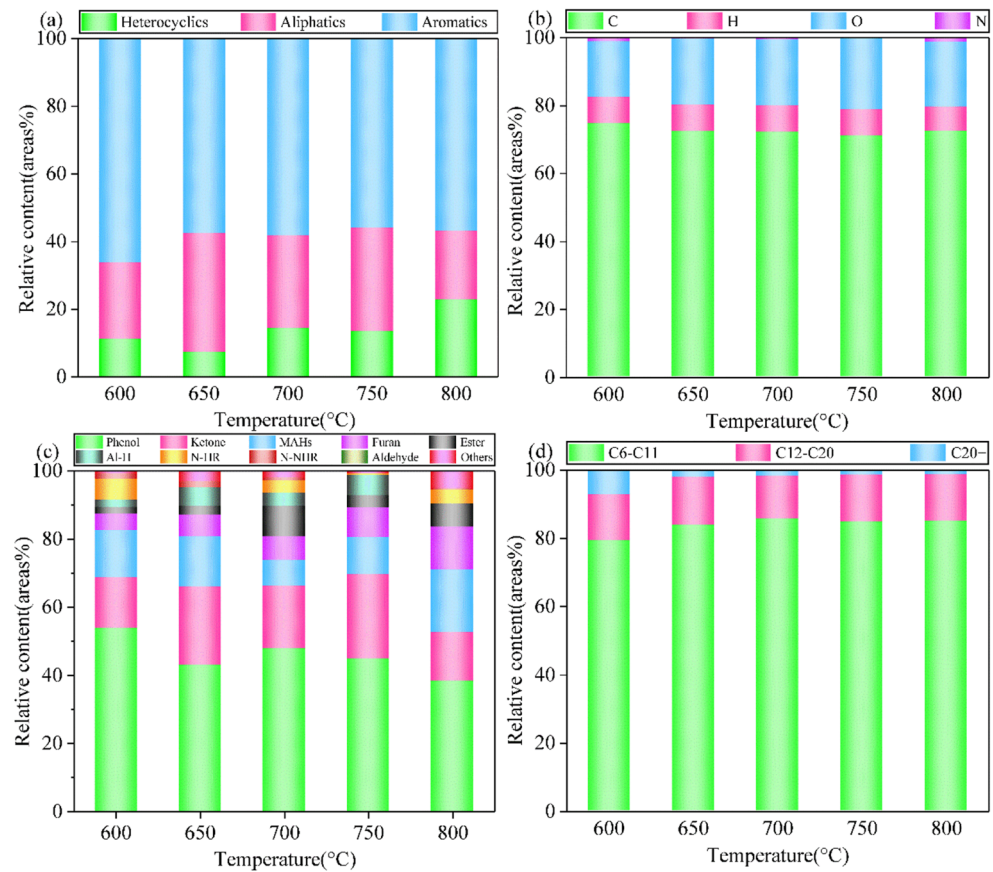
It can be seen from Fig. 4a the content of aromatics is always higher in in-situ groups than ex-situ groups. Meanwhile, the addition of CaO has significantly improved the content of aromatics compounds. The result showed that the content of aromatics compounds up to 85.32% in CaO-i group, while the maximum value in char-i group was only 61.99 %. It might be due to calcium-based catalysts promoted the aromatization of aliphatics and generated a large number of aromatics (Luo, et al. 2020). However, compared with CaO-i group, the char-CaO-i group caused the yield of aromatics decreased, but heterocyclics increased. It might be due to char promoted cyclization to form heterocyclics. Specifically, it may be due to the strength of ionic bond may affect the yield of aromatics, so, char with relatively weak ionic bonds can decrease the yield of aromatics. Meanwhile, Ohtsuka and Asami have pointed out that the additions of CaO can improve the qualities of PO because of the fine CaO particles with high reactive sites Shie et al. (2004a, b).

Figure 4b shows the relative content of C, H, O, and N under different conditions. The relative contents of C and H have little change, but the contents of O and N have changed obviously between in-situ and ex-situ catalytic pyrolysis. The maximum difference in the relative content of O was 12.07% between CaO-e and CaO-i groups; it indicated that Ca<sup>2+</sup> can promote the fracture of oxygen-containing functional groups which reform of light gas at 700 °C (Khan and Seshadri 1991). The O/C molar ratios of CaO-i group were the lowest (0.03), which demonstrated that CaO was beneficial to increase the saturation and calorific value of liquid products (Ellis, et al. 2015; Jones, et al. 2005).

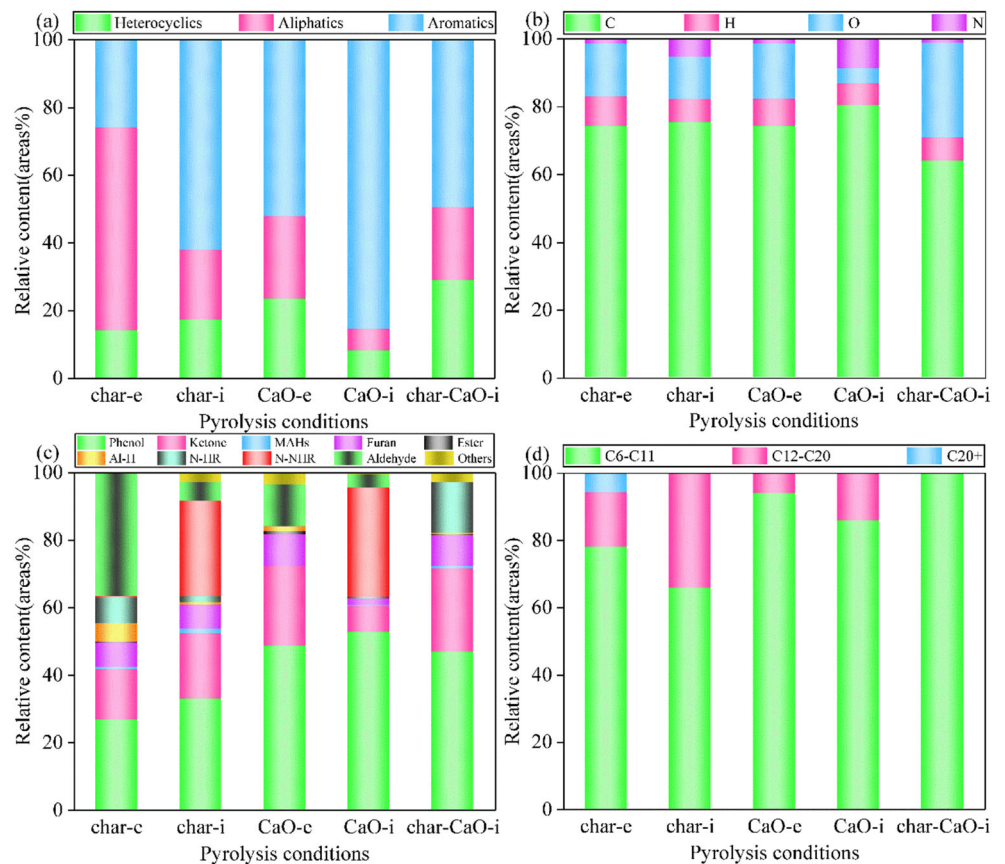
As performed in Fig. 4c, the products distribution was dominated by phenol and followed by ketone and furan; meanwhile, the total content reached from 48.94 to 81.69%. Phenol primarily originated from the decomposition of macromolecular aromatic compounds. Compared with char, the CaO can decompose of the aldehyde more efficiently, which might be due to CaO can easily break the carbon-oxygen double bond on the aldehyde group(-CHO). Meanwhile, the content of N-containing non-heterocyclic compounds (N-NHR) changed significantly between in-situ and ex-situ. The results showed that char and CaO can be easily fixed the nitrogen on the branch chain of the ring compound in char-CaO-i group.

The distribution of different carbon numbers in PO is shown in Fig. 4d. The contents of C6-C11 (gasoline fraction)

**Fig. 3** Distribution of PO compounds in temperature gradient pyrolysis experiments. **a** Heterocyclics, aliphatics, and aromatics contents of PO. **b** Carbon, hydrogen, oxygen, nitrogen contents of PO. **c** Different functional compounds contents of PO. **d** Different carbon numbers contents of PO



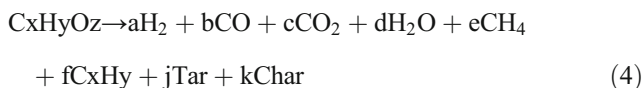
**Fig. 4** Distribution of PO compounds in catalytic pyrolysis experiments. **a** Heterocyclics, aliphatics, and aromatics contents of PO. **b** Carbon, hydrogen, oxygen, nitrogen contents of PO. **c** Different functional compounds contents of PO. **d** Different carbon numbers contents of PO



were the highest (65.85–99.71%), similar to that of gasoline and the contents of C11–C20 (diesel fraction) was relatively low. The highest content of C20+ was 5.81 % in char-e group, and other groups were 0%. CaO can increase the content of C6–C11 significantly, and it indicated CaO can depolymerization of macromolecular compounds. The content of C6–C11 was reached maximum value (99.71 %) in char-CaO-i group, and it shows that CaO and char have a synergistic effect on depolymerization of macromolecular compounds.

### Pyrolysis gas (PG) characteristics

C<sub>x</sub>H<sub>y</sub>O<sub>z</sub> can be represented as OS, and the pyrolysis reaction could happen as follows:



The relative contents of CO, H<sub>2</sub>, CH<sub>4</sub>, and CO<sub>2</sub> in PG were determined by GC. As shown in Fig. 5, the main components of PG were H<sub>2</sub> and CO<sub>2</sub>, accounted for 61.25–79.78%. Compared to 600 °C, the relative contents of H<sub>2</sub> at 650, 700, 750, and 800 °C were increased by 14.78%, 12.29%, 10.24%, and 1.75%, respectively. In addition, the relative contents of

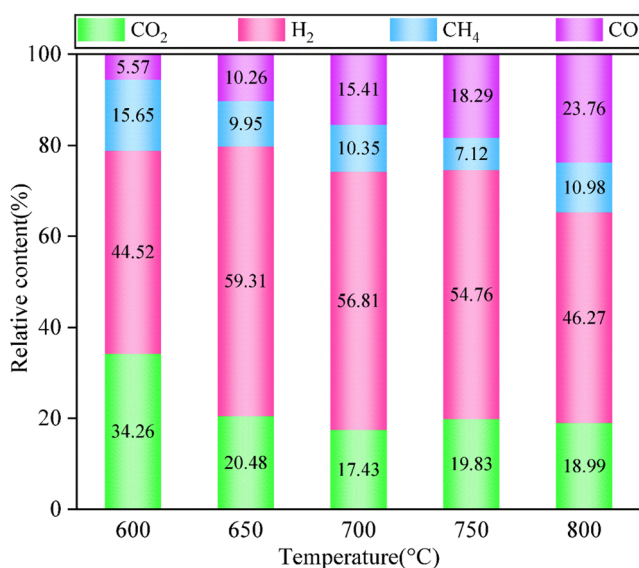


Fig. 5 Distribution of composition of PG in temperature gradient pyrolysis experiments

CO<sub>2</sub> were decreased by 13.78%, 16.83%, 14.43%, and 15.27%, respectively. These may be due to the promotion of dehydrogenation, decarboxylation, and decarbonylation at high temperature (Lin, et al. 2019).

The relative content of H<sub>2</sub> was approximate to maximum (59.30%) at 650 °C, but the gas yield was relatively low. This phenomenon may be due to incomplete pyrolysis of OS at this temperature, and some volatile hydrocarbons were converted into PS as a result of thermal dehydrogenation (Huang, et al. 2015). An increasing trend in CO yield was observed with the increasing temperature, and it was due to thermal cracking of carbonyl groups (C=O), ether bond (C–O–C), and the cracking of volatile compounds including oxygen heterocyclic compounds and ketones (Li, et al. 2018).

At 700 °C, the relative content of CO<sub>2</sub> in the PG was the lowest (17.43 %), and the relative content of combustible gas (H<sub>2</sub>, CH<sub>4</sub>, and CO) was the highest (82.57%). So, the PG had the best combustion performance and the highest calorific value and the catalytic pyrolysis experiments operated at this temperature.

Fig. 6 shows the PG compositions diagram of OS obtained under different catalytic conditions at 700 °C. It can be seen from Fig. 6 that the relative content of H<sub>2</sub> was lowest (16.24%), and the relative content of CO was highest (32.03 %) in the char-e group. These may be due to the char can break C–H of C<sub>n</sub>H<sub>m</sub> and C=O of CO<sub>2</sub> and generated H<sub>2</sub> and CO. Particularly, the relative content of CO increases significantly, and the reaction was as Eq. (5). Compared with char-e group, in the char-i group, the relative content of CO<sub>2</sub> slightly increased (1.19 %), and the relative content of H<sub>2</sub> increased significantly (29.10%). However, the relative content of CH<sub>4</sub> decreased significantly (20.83%). On the one hand, this may be due to char can break the bond of O–H in H<sub>2</sub>O and break the

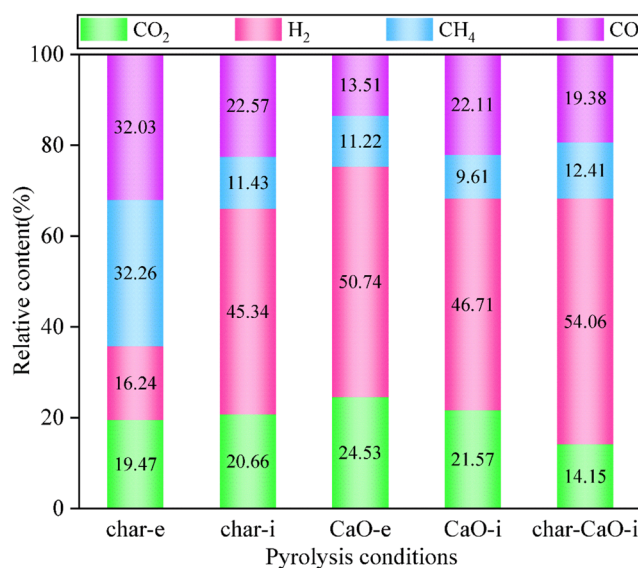


Fig. 6 Distribution of composition of PG in catalytic pyrolysis experiments

bond of C-H in CH<sub>4</sub>; the reaction was as Eq. (6). On the other hand, this may be due to the bond energy of C-C was lower than that of the C-H bond; the C-C bond could be easily broken in the volatile matter in char-e group. Meanwhile, the cleavage of alkanes which contains more carbon atoms will form new kinds of alkanes (short fragment alkanes and long fragment alkenes), and the free radicals formed can mutually combine freely with hydrogen atoms (Chen, et al. 2016). It indicated that the char may capture hydrogen atoms in the OS to form to CH<sub>4</sub>. So, the relative content of CH<sub>4</sub> in char-e group was higher than that in the char-i group, and the relative content of H<sub>2</sub> shown the opposite trend, as shown in reaction Eq. (7).

The relative content of CO<sub>2</sub> in CaO-e group was little higher than CaO-i group. It may due to CaO prompted the water-gas shift reaction Eq. (8) to produce more H<sub>2</sub> and a little of CO<sub>2</sub>. The yield of CO was increased especially in CaO-i group because of CaO could promote the decarbonylation reaction through break the C-O bond of organic substances (Xu, et al. 2017). Meanwhile, it may due to the product of carboxyl group cracking converted CO<sub>2</sub> into CO, as shown in reaction Eq. (9) (Li et al., 2018; Yuan et al., 2012). Compared with char, CaO had a better catalytic effect on the production of H<sub>2</sub>. The yield of H<sub>2</sub> derived from the CaO catalyst groups was higher than char catalyst groups; it has been reported that alkaline-earth metals could promote the production of H<sub>2</sub> by catalyzing hydrogen production reactions and CaO may have better catalytic performance to pyrolysis of the OS (Hu, et al. 2015; Li, et al. 2018).

In char-CaO-i group, the dual-catalyst has a significant synergistic effect on the production of H<sub>2</sub>. Char at 700 °C can promote the bond-breaking reformation of gaseous water molecules and CH<sub>4</sub>, and finally generated H<sub>2</sub> and CO<sub>2</sub>, the reaction was as Eq. (6). CaO can promote the reaction of carbon in PS with gaseous water molecules to generate CO and H<sub>2</sub>; the reaction was shown in Eq. (10). At the same time, the CO<sub>2</sub> produced by the reaction of Eq. (6) was reacted with carbon in PS under the action of CaO to produce CO; the reaction was shown in Eq. (9). Therefore, the relative content of combustible gas up to 85.85%, the PG kept at the highest combustion performance in char-CaO-i group. Specifically, the relative content of H<sub>2</sub> increased significantly, CO increased a little, but CO<sub>2</sub> was decreased.

### Pyrolysis solid (PS) characteristics

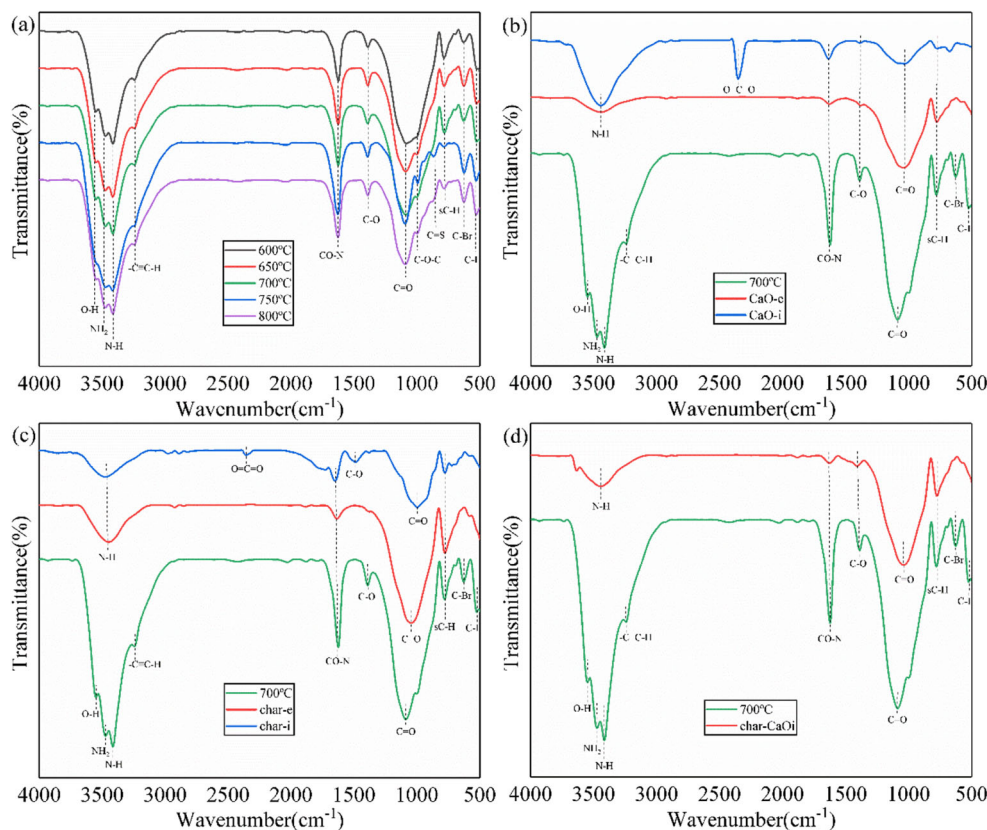
From Fig. 7(a), it can be seen that the stretching vibration peaks observed at about 3600 cm<sup>-1</sup> can be assigned to existence of free and intermolecular bonded O-H groups, and the stretching peak of O-H increased from 600 to 750 °C, while the transmittance of O-H peak decreased significantly at 800 °C. The O-H bond had strong polarity when the temperature at

750 °C, which indicated the presence of some isolated phenolic hydroxyl groups in the PS at 750 °C (Sharma, et al. 2002). The stretching vibration peaks observed at about 1600 cm<sup>-1</sup> can be assigned to CO-N, and the strongest stretching vibration at 750 °C. This may be that the NH<sub>2</sub> group was more likely to combine with C=O at this temperature and a new CO-N group was formed. The C=O stretching vibration intensity decreased significantly at 750 °C; this phenomenon just explained the reason for the formation of CO-N, and it indicated that C=O was compatible with the presence of acids and aldehydes (Xu, et al. 2017). The oxygen-containing groups (CO-N, C-O, C=O, and C-O-C) from 1800 to 900 cm<sup>-1</sup> were almost not changed at different temperatures. The peak from 750 to 550 cm<sup>-1</sup> corresponded to inorganic and organic halogens compounds or sulfur-containing substances in the PS, and it had little affected by temperature (Gao, et al. 2017).

According to Fig. 7b, the absorption peaks observed at about 3400, 1600, and 1080 cm<sup>-1</sup> were N-H, CO-N, and C=O, respectively, and they were significantly weakened both in CaO-e and CaO-i groups. Especially in CaO-e group, the N-H deformation vibration peak almost disappeared, and this may be caused by NH<sub>2</sub> asymmetric stretching. The absorption peak strength of CO-N around at 1600 cm<sup>-1</sup> decreased significantly in CaO-e and CaO-i groups. This could be due to the inhibition of the unsaturated absorption of NH<sub>2</sub> at the α or β position of the C=O bond on the aliphatic open-chain ketones. The absorption peak strength of C=O at about 1080 cm<sup>-1</sup> decreased significantly in CaO-e group. This may be due to the conjugation of the C=O bonds with α, β double bonds or aryl groups under the catalysis of CaO to shift the the C=O absorption band to a slightly lower wavenumber position and reduce its strength. In addition, the O=C=O characteristic peak at about 2350 cm<sup>-1</sup> may be due to the fixed of CO<sub>2</sub> by the CaO catalyst in PS.

According to Fig. 7c, a result similar to that of Fig. 7b was obtained, but in char-i group, a slightly absorption peak appeared at about 2350 cm<sup>-1</sup> in the PS and the stretching vibration of O=C=O was shown at here. The absorption peak around at 1500 cm<sup>-1</sup> to 1400 cm<sup>-1</sup> was the characteristic peak of C-O. Compared with 700 °C, the C-O peak was relatively broad, and its position was offset about 100 cm<sup>-1</sup> in the char-i group. The absorption at this region was considered to be related to the stretching vibration of only a C-O link. Figure 7d was an infrared comparison chart of pyrolysis of OS at 700 °C and in char-CaO-i group. According to Fig. 7d, the absorption peak strength of CO-N and C-O around at 1600 cm<sup>-1</sup> and 1400 cm<sup>-1</sup>, respectively, decreased significantly in char-CaO-i group. These may be due to the synergistic effect of char and CaO, so the bond breakage of CO-N and C-O were more likely to occur. As can be seen from Fig. 7, compared with temperature gradient

**Fig. 7** Fourier transform infrared spectra (FT-IR) of PS in pyrolysis of OS experiment. **a** Infrared spectrum of PS in temperature gradient experiment. **b** Infrared spectrum of PS in CaO catalytic pyrolysis experiment. **c** Infrared spectrum of PS in char catalytic pyrolysis experiment. **d** Infrared spectrum of PS in char-CaO catalytic pyrolysis experiment



pyrolysis experiments, char and calcium oxide show similar effects, and they can inhibit the formation of nitrogen-containing radical groups on the surface of PS in the catalytic pyrolysis experiments.

**Conclusion**

The catalytic pyrolysis experiment of OS which use CaO and char reveals the relationship of different catalytic conditions which were carried out in a fixed-bed reactor. The effects of catalyst on the products were investigated, and the possible reaction mechanism was discussed. At 700 °C, the PG has the highest combustible gas composition, and it has the best combustion performance. Meanwhile, PO has the lowest oxygen content and excellent industrial application potential. CaO and char have opposite effects on the production of aromatics and aliphatics compounds in PO. In in-situ groups, char and CaO are beneficial to the production of H<sub>2</sub> and CO, respectively. In ex-situ groups, char and CaO are beneficial to the production of CH<sub>4</sub>, CO, and H<sub>2</sub>, respectively. In char-CaO-i group, CaO and char have a synergistic effect on the depolymerization of macromolecular compounds in the PO. At the same time, they can weaken the nitrogen fixation performance on the PS surface. The two catalysts have excellent pyrolysis performance

under different pyrolysis conditions and have high social value.

**Acknowledgements** We acknowledge the Hunan Kegou Environmental Protection Technology Co., Ltd. and ACME (Advanced Corporation for Materials & Equipments) for their company support in equipment modification.

**Author contribution** Zhi Zhou, Nan Zhou, and Wei Luo designed the research; Qian He and Sheng-xiong Huang performed the experiments; Qian He, Yi-feng Su, and Mao Xia did data analysis and wrote the paper. All authors read and approved the final manuscript.

**Funding** This research is supported by Science and Technology project of Changsha (No. kh1801219), Huxiang high level talent gathering project (2019RS1077), National Natural Science Foundation of China (Grant No. 21706060, 51703061, 51974123), Natural Sciences Foundation of Hunan Province, China (Grant No. 2017JJ3103), the Distinguished Youth Foundation of Hunan Province (Grant No. 2020JJ2018), the Natural Sciences Foundation of Hunan Agricultural University, China (Grant No. 19QN11), and Hunan Provincial Engineering Technology Research Center for Optical Agriculture (Grant No. 2018TP2003).

**Declarations**

**Ethics approval** Not applicable

**Consent to participate** Not applicable



**Consent for publication** Not applicable

**Competing interests** The authors declare no competing interests.

## References

- Abdel Azim A-AA, Abdul-Raheim A-RM, Kamel RK, Abdel-Raouf ME (2011) Demulsifier systems applied to breakdown petroleum sludge. *J Pet Sci Eng* 78(2):364–370. <https://doi.org/10.1016/j.petrol.2011.07.008>
- Al-Zahrani SM, Putra MD (2013) Used lubricating oil regeneration by various solvent extraction techniques. *J Ind Eng Chem* 19(2):536–539. <https://doi.org/10.1016/j.jiec.2012.09.007>
- Cameotra SS, Singh P (2008) Bioremediation of oil sludge using crude biosurfactants. *Int Biodeterior Biodegrad* 62(3):274–280. <https://doi.org/10.1016/j.ibiod.2007.11.009>
- Check GR, Mowla D (2013) Theoretical and experimental investigation of desalting and dehydration of crude oil by assistance of ultrasonic irradiation. *Ultrason Sonochem* 20(1):378–385. <https://doi.org/10.1016/j.ultsonch.2012.06.007>
- Chen Z, Hu M, Cui B, Liu S, Guo D, Xiao B (2016) The effect of bioleaching on sewage sludge pyrolysis. *Waste Manag* 48:383–388. <https://doi.org/10.1016/j.wasman.2015.10.002>
- Chen X, Chen Y, Yang H, Chen W, Wang X, Chen H (2017) Fast pyrolysis of cotton stalk biomass using calcium oxide. *Bioresour Technol* 233:15–20. <https://doi.org/10.1016/j.biortech.2017.02.070>
- Cheng S, Wang Y, Fumitake T, Kouji T, Li A, Kunio Y (2017) Effect of steam and oil sludge ash additive on the products of oil sludge pyrolysis. *Appl Energy* 185:146–157. <https://doi.org/10.1016/j.apenergy.2016.10.055>
- Egazar'yants SV, Vinokurov VA, Vutolkina AV, Talanova MY, Frolov VI, Karakhanov EA (2015) Oil sludge treatment processes. *Chem Technol Fuels Oils* 51(5):506–515. <https://doi.org/10.1007/s10553-015-0632-7>
- Elektorowicz M, Habibi S (2005) Sustainable waste management: recovery of fuels from petroleum sludge. *Can J Civ Eng* 32(1):164–169. <https://doi.org/10.1139/04-122>
- Ellis N, Masnadi MS, Roberts DG, Kochanek MA, Ilyushechkin AY (2015) Mineral matter interactions during co-pyrolysis of coal and biomass and their impact on intrinsic char co-gasification reactivity. *Chem Eng J* 279:402–408. <https://doi.org/10.1016/j.cej.2015.05.057>
- Fuentes-Cano D, Gómez-Barea A, Nilsson S, Ollero P (2013) Decomposition kinetics of model tar compounds over chars with different internal structure to model hot tar removal in biomass gasification. *Chem Eng J* 228:1223–1233. <https://doi.org/10.1016/j.cej.2013.03.130>
- Gao N, Quan C, Liu B, Li Z, Wu C, Li A (2017) Continuous pyrolysis of sewage sludge in a screw-feeding reactor: products characterization and ecological risk assessment of heavy metals. *Energy Fuel* 31(5):5063–5072. <https://doi.org/10.1021/acs.energyfuels.6b03112>
- Gilbert P, Ryu C, Sharifi V, Swithenbank J (2009) Tar reduction in pyrolysis vapours from biomass over a hot char bed. *Bioresour Technol* 100(23):6045–6051. <https://doi.org/10.1016/j.biortech.2009.06.041>
- Hou S-S, Chen M-C, Lin T-H (2014) Experimental study of the combustion characteristics of densified refuse derived fuel (RDF-5) produced from oil sludge. *Fuel* 116:201–207. <https://doi.org/10.1016/j.fuel.2013.08.001>
- Hu G, Li J, Zeng G (2013) Recent development in the treatment of oily sludge from petroleum industry: a review. *J Hazard Mater* 261:470–490. <https://doi.org/10.1016/j.jhazmat.2013.07.069>
- Hu S, Jiang L, Wang Y, Su S, Sun L, Xu B, He L, Xiang J (2015) Effects of inherent alkali and alkaline earth metallic species on biomass pyrolysis at different temperatures. *Bioresour Technol* 192:23–30. <https://doi.org/10.1016/j.biortech.2015.05.042>
- Huang Q, Mao F, Han X, Yan J, Chi Y (2014) Characterization of emulsified water in petroleum sludge. *Fuel* 118:214–219. <https://doi.org/10.1016/j.fuel.2013.10.053>
- Huang Q, Wang J, Qiu K, Pan Z, Wang S, Chi Y, Yan J (2015) Catalytic pyrolysis of petroleum sludge for production of hydrogen-enriched syngas. *Int J Hydrog Energy* 40(46):16077–16085. <https://doi.org/10.1016/j.ijhydene.2015.09.139>
- Iliopoulou EF, Stefanidis SD, Kalogiannis KG, Delimitis A, Lappas AA, Triantafyllidis KS (2012) Catalytic upgrading of biomass pyrolysis vapors using transition metal-modified ZSM-5 zeolite. *Appl Catal, B* 127:281–290. <https://doi.org/10.1016/j.apcatb.2012.08.030>
- Jin Y, Zheng X, Chu X, Chi Y, Yan J, Cen K (2012) Oil Recovery from oil sludge through combined ultrasound and thermochemical cleaning treatment. *Ind Eng Chem Res* 51(27):9213–9217. <https://doi.org/10.1021/ie301130c>
- Jin J, Li Y, Zhang J, Wu S, Cao Y, Liang P, Christie P (2016) Influence of pyrolysis temperature on properties and environmental safety of heavy metals in biochars derived from municipal sewage sludge. *J Hazard Mater* 320:417–426. <https://doi.org/10.1016/j.jhazmat.2016.08.050>
- Jones JM, Kubacki M, Kubica K, Ross AB, Williams A (2005) Devolatilisation characteristics of coal and biomass blends. *J Anal Appl Pyrolysis* 74(1-2):502–511. <https://doi.org/10.1016/j.jaap.2004.11.018>
- Karamalidis AK, Voudrias EA (2007) Cement-based stabilization/solidification of oil refinery sludge: leaching behavior of alkanes and PAHs. *J Hazard Mater* 148(1-2):122–135. <https://doi.org/10.1016/j.jhazmat.2007.02.032>
- Khan MR, Seshadri K (1991) Compositional changes in the mild gasification liquids produced in the presence of calcium compounds. *Fuel Process Technol* 27:83–94. [https://doi.org/10.1016/0378-3820\(91\)90010-a](https://doi.org/10.1016/0378-3820(91)90010-a)
- Leonard SA, Stegemann JA (2010) Stabilization/solidification of petroleum drill cuttings. *J Hazard Mater* 174(1-3):463–472. <https://doi.org/10.1016/j.jhazmat.2009.09.075>
- Li T, Guo F, Li X, Liu Y, Peng K, Jiang X, Guo C (2018) Characterization of herb residue and high ash-containing paper sludge blends from fixed bed pyrolysis. *Waste Manag* 76:544–554. <https://doi.org/10.1016/j.wasman.2018.04.002>
- Lin B, Huang Q, Ali M, Wang F, Chi Y, Yan J (2019) Continuous catalytic pyrolysis of oily sludge using U-shape reactor for producing saturates-enriched light oil. *Proc Combust Inst* 37(3):3101–3108. <https://doi.org/10.1016/j.proci.2018.05.143>
- Liu J, Jiang X, Zhou L, Wang H, Han X (2009) Co-firing of oil sludge with coal-water slurry in an industrial internal circulating fluidized bed boiler. *J Hazard Mater* 167(1-3):817–823. <https://doi.org/10.1016/j.jhazmat.2009.01.061>
- Lu T, Yuan H, Wang Y, Huang H, Chen Y (2015) Characteristic of heavy metals in biochar derived from sewage sludge. *J Mater Cycles Waste Manage* 18(4):725–733. <https://doi.org/10.1007/s10163-015-0366-y>
- Luo W, Su Y-F, Hu Q, Yin H-L, Wang S, Ao L-J, Wen X-X, Huang S-X, Zhou N, Zhang W, Zhou Z (2020) Effect of calcium-based catalysts on pyrolysis liquid products from municipal sludge. *BioEnergy Res* 13(3):887–895. <https://doi.org/10.1007/s12155-020-10109-8>
- Min Z, Yimsiri P, Asadullah M, Zhang S, Li C-Z (2011) Catalytic reforming of tar during gasification. Part II Char as a catalyst or as a catalyst support for tar reforming. *Fuel* 90(7):2545–2552. <https://doi.org/10.1016/j.fuel.2011.03.027>
- Mrayyan B, Battikhi MN (2005) Biodegradation of total organic carbons (TOC) in Jordanian petroleum sludge. *J Hazard Mater* 120(1-3):127–134. <https://doi.org/10.1016/j.jhazmat.2004.12.033>

- Rodriguez IM, Laresgoiti MF, Cabrero MA, Torres A, Chomon MJ, Cabellero B (2001) Pyrolysis of scrap tyres. *Fuel Process Technol* 72:9–22. [https://doi.org/10.1016/S0378-3820\(01\)00174-6](https://doi.org/10.1016/S0378-3820(01)00174-6)
- Salman CA, Schwede S, Thorin E, Yan J (2017) Enhancing biomethane production by integrating pyrolysis and anaerobic digestion processes. *Appl Energy* 204:1074–1083. <https://doi.org/10.1016/j.apenergy.2017.05.006>
- Sharma RK, Wooten JB, Baliga VL, Martoglio-Smith PA, Hajaligol MR (2002) Characterization of char from the pyrolysis of tobacco. *J Agric Food Chem* 50(4):771–783. <https://doi.org/10.1021/jf0107398>
- Shen Y, Zhao P, Shao Q, Takahashi F, Yoshikawa K (2015) In situ catalytic conversion of tar using rice husk char/ash supported nickel-iron catalysts for biomass pyrolytic gasification combined with the mixing-simulation in fluidized-bed gasifier. *Appl Energy* 160:808–819. <https://doi.org/10.1016/j.apenergy.2014.10.074>
- Shie JL, Lin J-P, Chang C-Y, Lee D-J, Wu C-H (2003) Pyrolysis of oil sludge with additives of sodium and potassium compounds. *Resour Conserv Recycl* 39(1):51–64. [https://doi.org/10.1016/s0921-3449\(02\)00120-9](https://doi.org/10.1016/s0921-3449(02)00120-9)
- Shie J-L, Lin J-P, Chang C-Y, Lee D-J, Wu C-H (2004a) Oxidative thermal treatment of oil sludge at low heating rates. *Energy Fuel* 18:1272–1281. <https://doi.org/10.1021/ef0301811>
- Shie J-L, Lin J-P, Chang C-Y, Shih S-M, Lee D-J, Wu C-H (2004b) Pyrolysis of oil sludge with additives of catalytic solid wastes. *J Anal Appl Pyrolysis* 71(2):695–707. <https://doi.org/10.1016/j.jaap.2003.10.001>
- Song Q, H-y Z, W-l X, L-h S, Yang L, Yang D, Shu X (2018) Effects of various additives on the pyrolysis characteristics of municipal solid waste. *Waste Manag* 78:621–629. <https://doi.org/10.1016/j.wasman.2018.06.033>
- Wang ZQ, Guo QJ, Liu XM, Cao CQ (2007) Low temperature pyrolysis characteristics of oil sludge under various heating conditions. *Energy Fuel* 21(2):957–962. <https://doi.org/10.1021/ef060628g>
- Wang D, Yuan W, Ji W (2011) Char and char-supported nickel catalysts for secondary syngas cleanup and conditioning. *Appl Energy* 88(5):1656–1663. <https://doi.org/10.1016/j.apenergy.2010.11.041>
- Wang N, Chen D, Arena U, He P (2017a) Hot char-catalytic reforming of volatiles from MSW pyrolysis. *Appl Energy* 191:111–124. <https://doi.org/10.1016/j.apenergy.2017.01.051>
- Wang J, Zhang B, Zhong Z, Ding K, Deng A, Min M, Chen P, Ruan R (2017b) Catalytic fast co-pyrolysis of bamboo residual and waste lubricating oil over an ex-situ dual catalytic beds of MgO and HZSM-5: Analytical PY-GC/MS study. *Energy Convers Manag* 139:222–231. <https://doi.org/10.1016/j.enconman.2017.02.047>
- Wu Z, Li Y, Xu D, Meng H (2019a) Co-pyrolysis of lignocellulosic biomass with low-quality coal: optimal design and synergistic effect from gaseous products distribution. *Fuel* 236:43–54. <https://doi.org/10.1016/j.fuel.2018.08.116>
- Wu Z, Ma C, Jiang Z, Luo Z (2019b) Structure evolution and gasification characteristic analysis on co-pyrolysis char from lignocellulosic biomass and two ranks of coal: Effect of wheat straw. *Fuel* 239:180–190. <https://doi.org/10.1016/j.fuel.2018.11.015>
- Xu X, Zhao B, Sun M, Chen X, Zhang M, Li H, Xu S (2017) Co-pyrolysis characteristics of municipal sewage sludge and hazelnut shell by TG-DTG-MS and residue analysis. *Waste Manag* 62:91–100. <https://doi.org/10.1016/j.wasman.2017.02.012>
- Yang Z, Cao J-P, Ren X-Y, Zhao X-Y, Liu S-N, Guo Z-X, Shen W-Z, Bai J, Wei X-Y (2019) Preparation of hierarchical HZSM-5 based sulfated zirconium solid acid catalyst for catalytic upgrading of pyrolysis vapors from lignite pyrolysis. *Fuel* 237:1079–1085. <https://doi.org/10.1016/j.fuel.2018.10.049>
- Yuan S, Z-h D, Z-j Z, X-l C, Yu G-s, Wang F-c (2012) Rapid co-pyrolysis of rice straw and a bituminous coal in a high-frequency furnace and gasification of the residual char. *Bioresour Technol* 109:188–197. <https://doi.org/10.1016/j.biortech.2012.01.019>
- Zhang S, Asadullah M, Dong L, Tay H-L, Li C-Z (2013) An advanced biomass gasification technology with integrated catalytic hot gas cleaning. Part II: Tar reforming using char as a catalyst or as a catalyst support *Fuel* 112:646–653. <https://doi.org/10.1016/j.fuel.2013.03.015>
- Zhao H, Song Q, Liu S, Li Y, Wang X, Shu X (2018) Study on catalytic co-pyrolysis of physical mixture/staged pyrolysis characteristics of lignite and straw over an catalytic beds of char and its mechanism. *Energy Convers Manag* 161:13–26. <https://doi.org/10.1016/j.enconman.2018.01.083>
- Zhao H, Li Y, Song Q, Liu S, Ma Q, Ma L, Shu X (2019) Catalytic reforming of volatiles from co-pyrolysis of lignite blended with corn straw over three different structures of iron ores. *J Anal Appl Pyrolysis* 144. <https://doi.org/10.1016/j.jaap.2019.104714>
- Zhou L, Jiang X, Liu J (2009) Characteristics of oily sludge combustion in circulating fluidized beds. *J Hazard Mater* 170(1):175–179. <https://doi.org/10.1016/j.jhazmat.2009.04.109>
- Zubaidy EAH, Abouelnasr DM (2010) Fuel recovery from waste oily sludge using solvent extraction. *Process Saf Environ Prot* 88(5):318–326. <https://doi.org/10.1016/j.psep.2010.04.001>

**Publisher's note** Springer Nature remains neutral with regard to jurisdictional claims in published maps and institutional affiliations.